Frequency Identification of Bridges Using Smartphones on Vehicles with Variable Features

Nima Shirzad-Ghaleroudkhani[1]; Qipei Mei[2]; and Mustafa Gül, A.M.ASCE[3]

Abstract: This paper presents a crowdsensing framework employing smartphones in monitoring populations of bridges in future smart cities. In this regard, because there are a variety of vehicles with different features traveling over the bridge at different speeds, it is critical to investigate the robustness of indirect monitoring methods against vehicle features. Therefore, an experimental study was performed, including two lab-scale bridges with different boundary conditions and a robot car that was capable of maintaining a variety of speeds and suspension systems. The proposed framework focuses on the identification of frequencies of the bridge using acceleration signals recorded on the car. It was demonstrated that by using a large set of passing cars with different features, the fundamental frequency of the bridge was captured. Successful identification of the deviation of fundamental frequencies between two bridges with relatively close frequency values proved that the framework is capable of detecting damage induced frequency changes of the bridge. Since this framework relies on the use of smartphones, it provides the opportunity to efficiently monitor a plethora of bridges in a metropolitan area with minimum cost. **DOI: 10.1061/(ASCE)BE.1943-5592.0001565**. © *2020 American Society of Civil Engineers*.

Author keywords: Bridge; Frequency analysis; Indirect monitoring; Bridge; Smart city; Smartphone.

Introduction

Urban population growth over recent decades has created complications in the management of urban cities (Graham 2010). To overcome such difficulties, the concept of Smart City was developed by employing smart sensing, computing, and communication technologies in urban management (Chourabi et al. 2012; Washburn et al. 2010). Applications of smart technologies in transportation infrastructure have been widely studied in the literature (Adeli and Jiang 2009; Glancy 2014; Xiong et al. 2012). Bridges, as key components of transportation networks, are prone to structural damage resulting in an irrecoverable financial and time loss (Ham et al. 2005). Many bridge structures in modern countries have reached their design life and need to be monitored and retrofitted to remain in service in a cost-effective manner. For example, according to the Canadian Infrastructural Report Card (CCA/CPWA/CSCE/FCM 2016), approximately 40% of bridges in Canada are in fair, poor, or very poor conditions. The sustainability of transportation networks relies on appropriate monitoring and maintenance operations on bridges. Therefore, structural health monitoring (SHM) techniques were proposed as a critical component of viable transportation networks (Wenzel 2008).

Traditionally, most of the proposed SHM methods required bridge instrumentation with fixed sensors installed on the bridge, for example, Catbas et al. (2008), Guan et al. (2019), Gül and Catbas (2009), Hoult et al. (2010), Hsieh et al. (2006), Ko and Ni (2005), and Wong (2004). The functionality and accuracy of these methods were demonstrated in those studies. However, the feasibility of employing such direct SHM methods on a large number of bridges is a major concern. Instrumentation of each bridge with fixed sensors and creating a data collection network is costly and time-consuming, and can not be employed on all bridges. Therefore, new SHM methods were suggested by focusing on sensors placed in passing vehicles as moving sensors, i.e., indirect monitoring of bridges.

Indirect bridge monitoring concept was first proposed by Yang et al. (2004). They performed dynamic analysis of vehicle–bridge interaction for a simple 2D beam model representing the bridge and a moving mass–spring system representing the vehicle. It was shown that the frequency of the bridge could be extracted from the vibration of the vehicle. Afterward, many studies followed indirect bridge monitoring (Malekjafarian et al. 2015), which are divided into analytical/numerical studies (Hattori et al. 2012; Hester and González 2017; Keenahan et al. 2014; OBrien et al. 2017; Yang and Chen 2016), lab-scale experiments (Cerda et al. 2014; Mei et al. 2019; Zhang et al. 2013), and real-life experiments (Kim and Lynch 2012; Lin and Yang 2005; Siringoringo and Fujino 2012). All these studies corroborated the fact that bridge dynamic response exists in the vibration of the passing vehicle and can be extracted to assess the bridge condition. Therefore, the instrumentation of vehicles with accelerometers might provide an effective source of monitoring many bridges within a city. More recently, an alternative way of employing indirect monitoring methods using the smartphones of passengers in vehicles was proposed by several research groups as discussed in the following.

In the context of smart cities, smartphones are critical devices because they provided valuable crowdsensing data. They have important sensors, including accelerometer, gyroscope, and GPS, which could be used in the monitoring of different structures (Feng et al. 2015; Kong et al. 2018; Morgenthal et al. 2018;

[1]Graduate Student, Dept. of Civil and Environmental Engineering, Univ. of Alberta, Edmonton, AB, Canada T6G 1H9. Email: shirzadg@ualberta.ca

[2]Graduate Student, Dept. of Civil and Environmental Engineering, Univ. of Alberta, Edmonton, AB, Canada T6G 2W2. Email: qipei@ualberta.ca

[3]Associate Professor, Dept. of Civil and Environmental Engineering, Univ. of Alberta, Edmonton, AB, Canada T6G 1H9 (corresponding author). ORCID: https://orcid.org/0000-0002-7750-0906. Email: mustafa.gul@ualberta.ca

Note. This manuscript was submitted on May 23, 2019; approved on December 31, 2019; published online on May 6, 2020. Discussion period open until October 6, 2020; separate discussions must be submitted for individual papers. This paper is part of the ***Journal of Bridge Engineering***, © ASCE, ISSN 1084-0702.

Ozer and Feng 2016, 2017; Zhao et al. 2017). Regarding transportation networks, smartphones previously proved to be an effective tool to estimate traffic incidents, such as congestions or accidents (Bhoraskar et al. 2012; Händel et al. 2014; Mohan et al. 2008). However, their application to indirect SHM had not been investigated until recent studies showed that smartphones could be used as reliable sensors to collect acceleration data and apply them into indirect health monitoring techniques to assess bridge conditions. Mei and Gül (2019) proposed an indirect damage detection method based on mel frequency cepstral coefficients and used a smartphone to detect multiple damage states on a lab-scale bridge model. They showed, to the best of our knowledge, for the first time in the literature that the damage in the bridge model could be identified using the smartphone on a car model even if the speed, weight, and suspension of the car were varied between experiments. In another study, Matarazzo et al. (2018) performed a real-life experiment to investigate the possibility of capturing bridge frequencies using smartphones. These studies arrived at the same conclusion that the recorded vibration of the vehicle is highly dominated by vehicle features, such as suspension, mass, and speed.

Previously, many experiments studied the effect of car features on the frequency spectrum of the vehicle. Most of the past studies on indirect health monitoring of bridges were conducted using dedicated professional accelerometers placed in the vehicles to collect data from the car, while this study focuses on using smartphones as data collecting devices in future smart cities. Li et al. (2019) studied the effect of speed on the frequency content recorded on the cars passing over the bridge using a lab-scale test. They concluded that lower speeds benefits the process of frequency identification. A similar conclusion was made in another study by Kim et al. (2011). However, the car models in both studies were not motorized, while the data in our experiments showed that the main effect of the change in the speed of the car on the spectrum was due to the change in the revolving speed of the motor, which is also expected in real-life practice. In another study, Mei et al. (2019) conducted laboratory experiments where both speed and suspension stiffness of the car were considered. However, the damage detection method employed in that study did not focus on the modal analysis of the acceleration data.

Regarding large-scale indirect monitoring of populations of bridges in smart cities, where there are different vehicles with different features traveling at different speeds, it is vital to investigate the robustness of indirect monitoring methods using smartphones against vehicle features. Therefore, this study focused on the application of smartphones in different cars traveling at different speeds to capture frequencies of the bridge. Several laboratory experiments were conducted using two experimental bridge models with different support conditions, and a robot car model capable of changing suspension springs and traveling speeds. In total, three spring types and three speeds were applied to the car, resulting in nine combinations. The experiment consisted of three stages. First, vibration analysis of the bridge was conducted to extract the natural frequencies of the bridge. Then, robot car vibration was analyzed to study the frequency spectrum of the car while moving on a rigid non-vibrating surface. Finally, the vibration of the car while moving on the bridge was studied. Comparing the results of these three stages provided the possibility of investigating the robustness of using smartphones to capture bridge frequencies against vehicle features.

Methodology

In this section, the fundamental notion of vehicle–bridge interaction and its application to this research will be explained. Then, the frequency domain analysis applied to the vibration signals will be described.

Vehicle–Bridge Interaction

Vehicle–bridge interaction is the main concept in indirect bridge monitoring. Owing to the dynamic interaction, vibrations of vehicle and bridge are coupled to each other. In other words, the vibration of a vehicle moving over a bridge consists of both the vehicle and the bridge vibration. One of the first studies to investigate this notion was performed by Yang and Yau (1997). In that study, a simple 2D beam model was used to model a bridge and a moving mass–spring system was considered as the vehicle. The following equation was derived in that paper:

$$\begin{cases} \bar{m}(x)u_b''(x,\,t) + E(x)I(x)u_b''''(x,\,t) = c(x,\,t) \\ m_v u_v''(t) + k_v[u_v(t) - u_b(x,\,t)] = 0 \end{cases} \tag{1}$$

where x = distance to the bridge end; t = time; v = speed of the vehicle; $\bar{m}(x)$ = distributed mass of the bridge per unit length; $E(x)$ and $I(x)$ = elastic modulus and moment of inertia of the bridge section, respectively; m_v and k_v = mass and stiffness of the vehicle; and $c(x,\,t)$ = contact force. Furthermore, u_b and u_v are the vertical displacements of the bridge and the vehicle relative to the equilibrium position, respectively. The first equation is the governing dynamic equilibrium of the bridge, and the second one is of the vehicle. As seen in Eq. (1), the dynamic response of the vehicle includes dynamic characteristics of the bridge which means using an appropriate signal processing technique, it would be possible to extract bridge dynamic features, e.g., frequencies, from the vibration of the vehicle. Although this model was simple and did not account for many challenges such as complicated vehicle model, road roughness, and environmental effects, the fact that the dynamic features of the bridge exist in the vibration of the vehicle still prevails.

Frequency Domain Analysis

In this research, the frequency content of the acceleration signal is calculated using an averaging method proposed by Welch (1967), here called averaged discrete Fourier transform (ADFT), by averaging Fourier transforms of the main signal over small windows. The discrete Fourier transform (DFT) is described as follows:

$$X[k] = \sum_{n=0}^{N-1} u_v''[n]e^{-j(2\pi/N)kn} \tag{2}$$

where u_v'' = the acceleration signal recorded on the vehicle as previously defined in Eq. (1), N = the number of data points in the signal, and X = the vector of DFTs, which is a complex vector containing amplitude and phase values. Moreover, k = an index representing step frequencies using the following equation:

$$f = \frac{k}{N}f_s \quad \text{for } 0 \le k \le N-1 \tag{3}$$

where f_s = sampling frequency. Applying Eq. (2) to the whole acceleration signal results in a highly fluctuated spectrum, which is not suitable for peak analysis. However, if the signal is divided into multiple segments and each segment is considered as a separate signal in the DFT process, followed by averaging all of the spectrums, the resulting spectrum will be smoother and more convenient for peak analysis. Among a variety of window functions proposed for selecting subsignals (Harris 1978),

the hamming window is considered in this study. In addition, selected windows are not mutually exclusive to account for the effect of the transition and a percentage of the window length is considered as an overlap. Therefore, the ADFT of the signal is calculated using the following equation:

$$\bar{X}[k] = \frac{1}{M}\sum_{m=1}^{M}\sum_{n=0}^{N-1} w_m[n]u_v''[n]e^{-j(2\pi/N)kn} \quad (4)$$

where w_m = function for mth window, and M = total number of windows calculated by

$$M = 1 + \frac{N - N_w}{(1-p)\cdot N_w} \quad (5)$$

where p = overlap percentage of the windows. In this paper, since the lengths of most acceleration signals are between 6 and 12 s, a 5 s hamming window and 75% overlap are considered. To increase the frequency resolution of the ADFT spectrum, all windows are zero padded to 10 s, resulting in a 0.1 Hz resolution. Furthermore, the acceleration signals from the smartphone are resampled by interpolation before being converted to the frequency domain. The reason is that the sampling intervals of smartphones might not be perfectly consistent and deviate from the preset value. Although the android application developed by the authors' research group (Mei and Gül 2019) significantly improves the stability of sampling frequency, resampling of the signal still increases the accuracy of the calculation.

To identify the most significant frequencies in each spectrum, a peak picking technique based on amplitude and prominence has been employed using MATLAB (2018). The prominence of a peak represents how the peak stands out due to its intrinsic height and location with respect to other adjacent peaks. A low but isolated peak can be more prominent than another one that is higher but is among a range of tall peaks. However, two equally prominent peaks with a substantial difference in the amplitude are not equally significant in a spectrum. Therefore, both the prominence and amplitude are considered as the criteria in this study. The amplitude and prominence values for all peaks in a spectrum are scaled to 100, and the peak score is defined as the average of its amplitude and prominence scores. This averaged score is then used as a criterion to quantify the significance of the peaks in the spectrum.

Experimental Setup

This section illustrates the material and devices used in this experiment. First, two bridge models will be described. Then, the features of the robot car will be explained. Finally, the instruments utilized to collect data during the experiment will be presented.

Bridge

In this study, two types of bridges, one pin–roller and one fixed–fixed support, are considered. For both bridges, hot rolled steel plates of W44, with the modulus of elasticity of 200 GPa, yield strength of 250 MPa, and ultimate strength of 310 MPa, are used. These plates are 2 m long and 330 mm wide. The thickness of the plates in two bridge types is different: a 12.7 mm thick plate is used for the pin–roller bridge setup whereas a 6.35 mm thick plate is used for the fixed–fixed bridge setup. The reason for this selection is that using the low thickness plate for a pin–roller support bridge results in a significant sag in the middle of the bridge, which prevents the speed of the robot car from being constant when traveling over the bridge. However, using a thick plate for the fixed–fixed support bridge intensively increases the stiffness and frequency of the bridge, which not only makes the bridge vibration negligible for the car but also makes the experiment unrealistic.

Fig. 1 shows the setup for the pin–roller bridge. Here, one pin support and one roller support are employed to carry the 12.7 mm thick plate. In Fig. 2, the pin–roller support structure is illustrated. Both supports have the same structure, except that the pin is prevented from moving horizontally while the roller is free to move. As shown, an approaching span is also considered for the first few seconds when the car accelerates and reaches the constant target speed. Furthermore, another plate is used at the end of the bridge so that the car completely leaves the bridge and then stops. An additional small thick plate is employed between the main span plate and the supports so that the approaching and end spans do not have any contact with the supports and, therefore, do not affect their free rotation.

Fig. 3 shows the setup for the fixed–fixed bridge. In this bridge, both supports are assumed to be completely fixed. To reach full fixity, two 25 cm long W10 × 54 steel profile beams are used as the supports, which are connected to the main span plate of 6.35 mm thick through four bolts on both sides, as shown in Fig. 4. In addition, to prevent the supports from moving horizontally, nine reinforced concrete blocks are used at both ends. Similar to the pin–roller bridge, two plates were used as the approaching and end spans.

Vehicle

In this study, a robot car was designed and built as shown in Figs. 5 and 6. This car consists of two identical rectangular aluminum plates of 350 ×125 mm^2 with a thickness of 3.1 mm. The motor

Fig. 1. Pin–roller bridge setup.

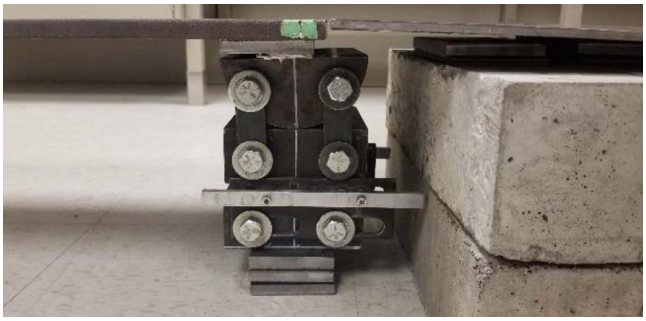

Fig. 2. Pin/roller support.

Fig. 3. Fixed–fixed bridge setup.

Fig. 4. Fixed support.

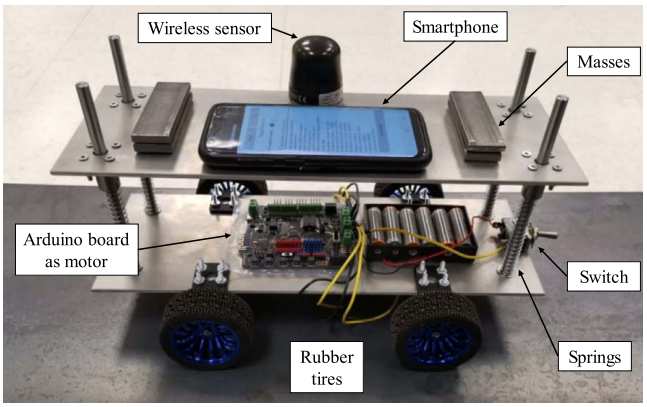

Fig. 5. The custom designed and custom built robot car.

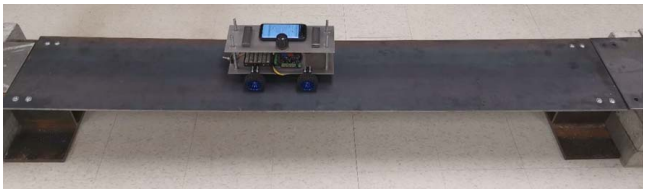

Fig. 6. Robot car on the fixed–fixed bridge.

and the wheels are connected to the bottom plate. Four aluminum rods with a radius of 4 mm and length of 15 cm surrounded by four springs are used to connect the bottom plate to the top plate, where the acceleration data are collected. Four linear bearings are connected to the top plate to ensure a smooth vertical movement on the springs.

The robot car in this study is capable of maintaining constant speeds between 0.2 and 0.4 m/s over flat surfaces or gentle slopes, therefore, three speed cases of 0.2, 0.3, and 0.4 m/s are considered here. In addition, to model three different suspension systems, three springs with stiffness values of 425, 615, and 726 N/m are employed. These springs are referred to as A, B, and C, respectively. The total mass of the top plate, including the smartphone and the sensor, is kept constant to 1.2 kg in all cases to make a better comparison with the effect of the suspension system on the spectrum of the passing car.

Instrumentation

To collect the acceleration from the car (Arduino, Somerville, MA), one smartphone, a Samsung Galaxy S8 (Samsung Electronics, Seoul, South Korea), with a sampling frequency of 400 Hz is used. Recording acceleration data from the smartphone is performed using an android app previously developed and used by Mei and Gül (2019), which provided the global vertical acceleration by using gyroscope and magnetometer in combination with an accelerometer. This app also applies sampling frequency correction to the recorded data. In addition to the smartphone, and to have a benchmark for comparison, one G-Link-200 (Lord Sensing Microstrain, Williston, VT) wireless accelerometer with a sampling frequency of 512 Hz is placed on the car, as shown in Fig. 5.

As verification, the acceleration data is collected from the bridge using three G-Link-200 wireless accelerometers with a sampling frequency of 512 Hz. To detect as many modes as possible, these sensors are mounted at midspan, quarter-span, and 3/8-span of both bridges, shown previously in Fig. 1, which guarantees to capture the vibration of at least the first four modes, based on the approximate mode shapes of the pin–roller and fixed–fixed beams.

Analysis

In this section, the analysis results will be discussed in three parts. First, a modal analysis of the bridge is conducted through free and tapping forced vibration tests. Then, the frequency content of the vibration of the car is investigated through nonmoving suspension tests and moving off-bridge tests. Finally, moving the car over the bridge is investigated.

Frequency Analysis of the Bridge

This section will provide an overview of the natural frequencies of two bridges considered in this study. First, a free vibration test is performed on each bridge by applying an initial deflection at 40% span length. Applying initial deflection to this point creates relatively larger amplitude vibration and excites at least the first four modes of both bridges. Fig. 7 shows the ADFT spectrum of the acceleration signals. The three columns in Fig. 7 represent three sensors located on the bridge, and two rows represent two considered bridges. The fundamental frequency of the pin–roller and fixed–fixed bridges are identified as 7.6 and 9 Hz, respectively. As expected, the amplitudes of the first and third modes are significant in the midspan sensor spectrum, while the second and fourth have a relatively major presence in the quarter-span sensor spectrum, especially in the fixed–fixed bridge. The other observation is that the first mode always has the largest amplitude in the free vibration test.

To identify higher mode frequencies with higher accuracy and larger amplitudes, another test is conducted using multiple tapping over different points along the bridge, to mimic ambient vibration tests. This way, higher modes of the bridge are excited and higher peaks appeared due to those modes, as shown in Fig. 8, which has a similar organization to that shown in Fig. 7. Considering the frequency range of 0–100 Hz, the second and third modes of the pin–roller bridge are 29.9 and 65.7 Hz, and the second to fifth modes of the fixed–fixed bridge are 26, 34.1, 50.3, and 69.8 Hz, respectively.

Frequency Analysis of the Robot Car

This section aims to experimentally investigate the frequency content of the vibration of the robot car taking into consideration three different suspension systems. First, the suspension system of the car is studied using a free vibration test, which is performed by applying an initial deflection to the top plate of the car when the car is in a stationary position. Since the damping

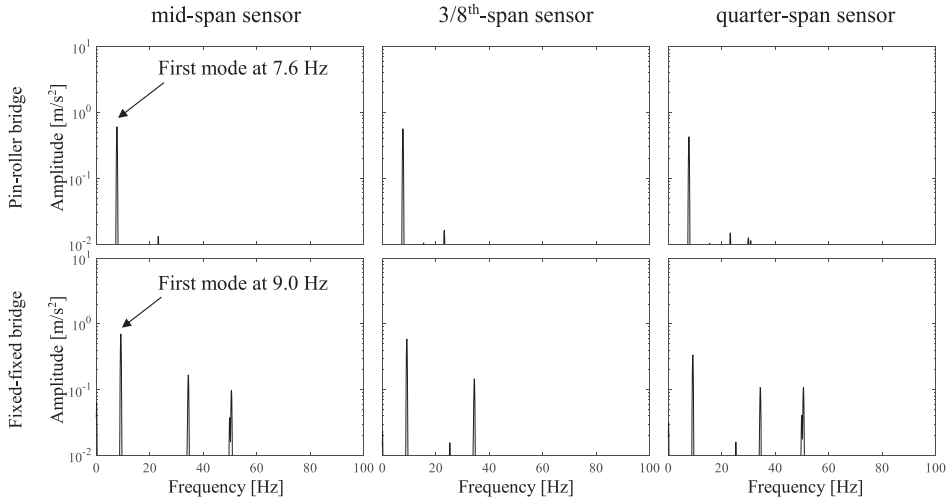

Fig. 7. ADFT spectrum of bridge sensors under free vibration of the bridge.

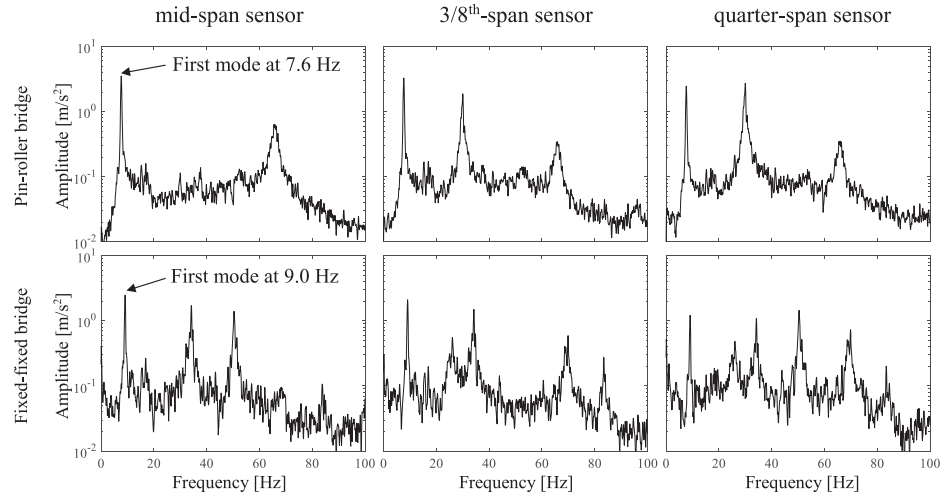

Fig. 8. ADFT spectrum of bridge sensors under tapping forced vibration of the bridge.

of the suspension system in this model is very large due to imperfections, the length of the free vibration signal is very short, i.e., approximately 2 s. Therefore, the ADFT analysis is conducted using smaller windows, resulting in a very smooth spectrum shown in Fig. 9, which has three rows representing three spring types used in this paper, and each graph contains two curves related to the sensor and the smartphone mounted on the car. As shown in Fig. 9, the frequency of the suspension system is visible in all three graphs and is equal to 3.9, 5, and 5.4 Hz, for three springs of A, B, and C, respectively. As expected, the frequency of the suspension system increases with the stiffness of the springs.

Another important observation in Fig. 9, is that the spectrum of the sensor and the smartphone agree when capturing the peak, but with different amplitudes. Since the main focus of this paper is to find the significant frequencies in the spectrum, it means that smartphones can be considered a reliable tool for this purpose.

After analyzing the suspension system, the vibration analysis of the car while moving on a rigid surface, i.e., off-bridge test, is conducted. This type of test is suitable for comparing the vibration of the same car moving on the bridge, to investigate the effect of the bridge on the car vibration. Fig. 10 shows the spectrum of the sensor and the smartphone mounted on the car under different conditions. Three columns in Fig. 10 illustrate the speed values of the car, while three rows represent different springs and, therefore, different suspension systems. As shown in Fig. 10, there are three major peak ranges visible in these graphs. Considering $v = 0.2$ m/s, there are multiple peaks at approximately 14, 30, and 54 Hz. However, these peaks change to 18.5, 34, and 67.5 in $v = 0.3$ m/s, and 22, 43, and 85 in $v = 0.4$ m/s, respectively. However, the columns shown in Fig. 10 prove that these peaks do not change with the suspension system of the car. Based on the results shown in Fig. 9, the frequencies of the suspension system are all below 10 Hz, which are not significantly excited in this experiment in Fig. 10. The reason is that unless there is a huge surface disruption, such as potholes, the suspension frequency would be noticeably less excited with respect to other sources of vibration, such as motor vibration or the moving frequency of the vehicle. In addition, similar to Fig. 9, this experiment corroborates the application of smartphones to detect the frequency content of the car.

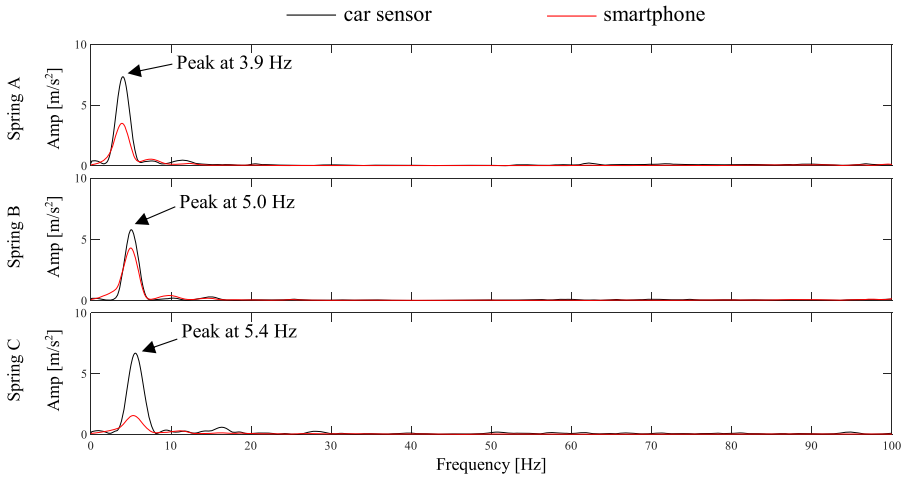

Fig. 9. ADFT spectrum of the car sensor and smartphone under suspension test using three different springs.

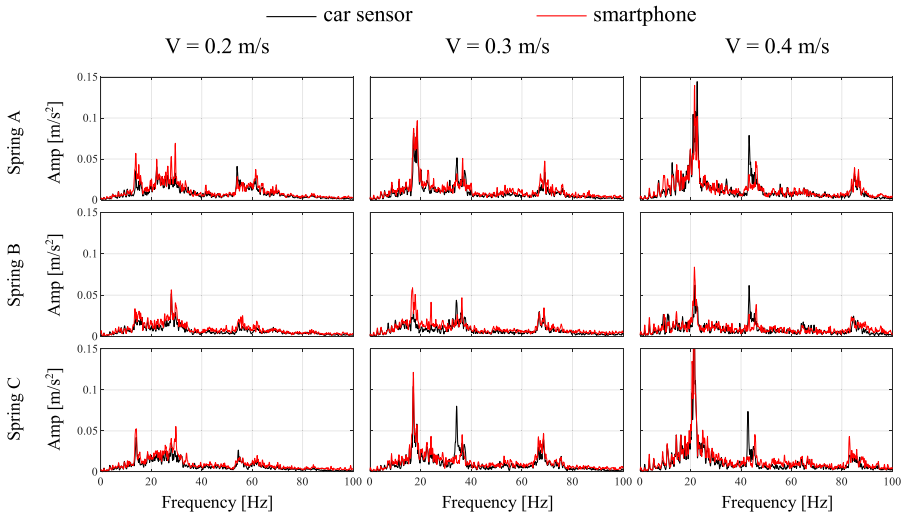

Fig. 10. ADFT spectrum of the car sensor and smartphone under off-bridge test using three different springs at three different speeds.

Frequency Analysis of the Robot Car Moving on the Bridge

In this section, the vibration recorded on the car while moving on the bridge is studied. Similar to the previous section of frequency analysis of the bridge, first the condition of the moving car as the only source of vibration, i.e., with no external force acting on the bridge, is considered. Then, along with the car moving, multiple tapping on different points on the bridge is applied, to account for larger vibrations of the bridge due to other forces, such as other cars or wind loads. Comparing the frequency contents of this section with those of the off-bridge experiment in the previous section makes it possible to identify the effect of bridge vibration on the recorded acceleration on the car.

Figs. 11 and 12 show the spectrums of the car moving over pin–roller and fixed–fixed bridges, respectively, while no external forces are acting on the bridge. The organization of both Figs. 11 and 12 is similar to Fig. 10 except that there are vertical dashed lines added to the graphs showing the first three frequencies of each bridge identified through the bridge experiments. Both Figs. 11 and 12 almost show the same pattern seen in the off-bridge analysis in Fig. 10, with the only difference that there is one extra relatively sharp peak below 10 Hz, close to the fundamental frequency of the bridge. In Fig. 11, the first peak in the first column, i.e., when $v = 0.2$ m/s, is equal to 7.3 Hz, while this peak changes to 7.2 and 7 Hz for $v = 0.3$ m/s and $v = 0.4$ m/s, respectively. This deviation from the exact bridge frequency, 7.6 Hz, verifies the previously shown phenomena of shifted frequency (Yang et al. 2004) of the bridge in the vibration of the car, which increases with the speed of the vehicle. Similarly, in Fig. 12, the identified frequencies of the bridge are 8.7, 8.6, and 8.4 for $v = 0.2$, 0.3, and 0.4 m/s, respectively, compared with the exact fundamental frequency of 9 Hz.

As shown in Figs. 11 and 12, it seems that higher modes are either not excited or their amplitude is very low when there is no other source of excitation except the moving car. In this experiment, the higher modes of the bridge, excited with relatively lower amplitudes, lie within the peaks of the car spectrum, excited with significantly larger amplitudes, and therefore, preventing those modes from being visible in the combined vibration spectrum. However, the fundamental frequency of the bridge is below 10 Hz, where there are no significant peaks visible in the off-bridge spectrum shown in Fig. 10.

In real-life situations, there are many sources of excitation acting simultaneously on the bridge, e.g., many cars moving in multiple lanes in similar or opposite directions, or the effects of winds, which results in larger vibration of the bridge and, therefore, the

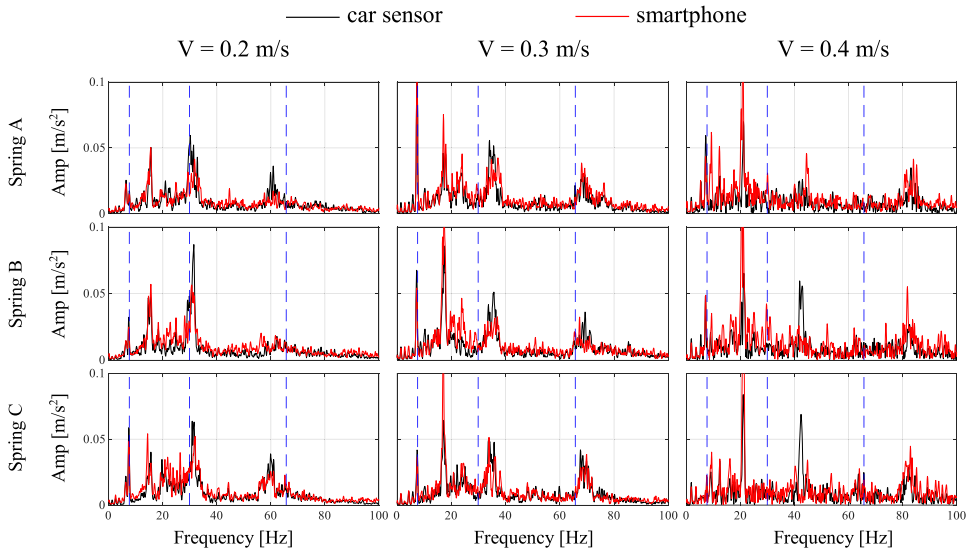

Fig. 11. ADFT spectrum of the car sensor and smartphone under free on-bridge test on the pin–roller bridge using three different springs at three different speeds.

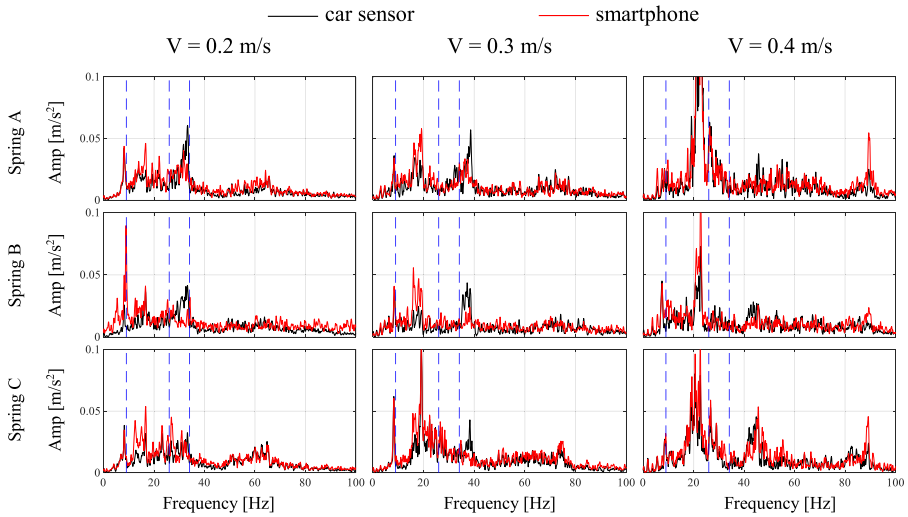

Fig. 12. ADFT spectrum of the car sensor and smartphone under free on-bridge test on the fixed–fixed bridge using three different springs at three different speeds.

stronger presence of its frequencies in the car spectrum. Hence, another set of experiments is conducted by tapping multiple points along the bridge while the car moves over the bridge. Figs. 13 and 14 show the spectrum of the car vibration during this experiment for pin–roller and fixed–fixed bridges, respectively. As expected, the presence of tapping forced excitation that mimics other real-life sources of excitation increases the bridge vibration, resulting in a clear significant peak close to the fundamental frequency of the bridge. In addition, in some cases for the pin–roller bridge and nearly all cases in the fixed–fixed bridge, the second mode of the bridge is present in the car spectrum.

The important conclusion from this section is that if there is a substantial difference between the frequencies of the bridge and different cars passing over the bridge, it is possible to detect the shifted fundamental frequency of the bridge using the acceleration signal of the car recorded on the smartphone. In addition, with sufficient vibration of the bridge, there is a potential that the second mode of the bridge can be captured. Moreover, it should be noted that, in future studies, the speed of the car while crossing the bridge can be easily obtained using the built-in GPS of smartphones and this information can be used to eliminate the effects of the speed on the identified frequencies.

Application to Bridge State Detection

This section focuses on the application of the proposed frequency analysis of smartphone data for assessing the changes in the structural condition of the bridge. Take into consideration a large number of smartphones, as sources of data, located on many cars with different features traveling over a bridge at different speeds. It is shown in this study that it is possible to capture at least the first shifted frequency of the bridge through frequency analysis of the acceleration signals recorded on smartphones. At this point, the main challenge is the damage detection capability of these types of signals.

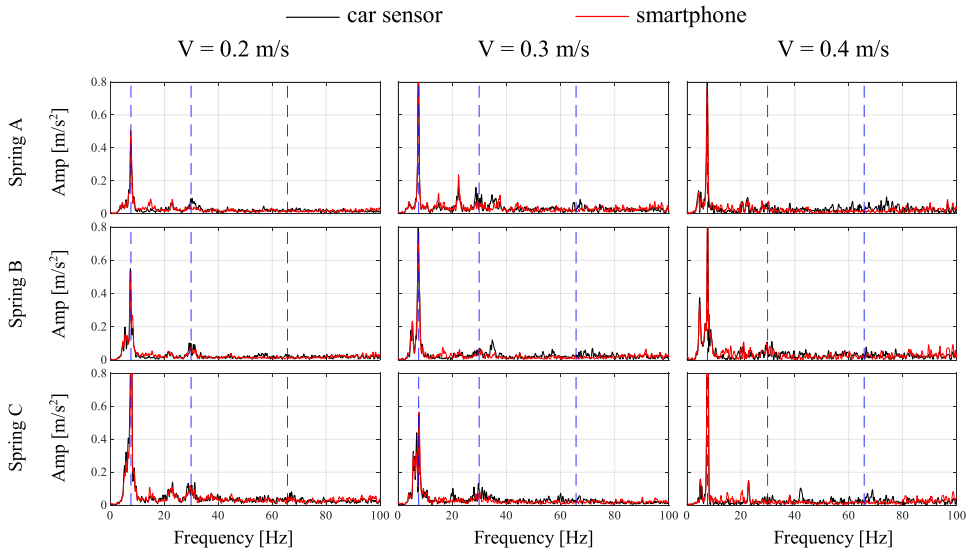

Fig. 13. ADFT spectrum of the car sensor and smartphone under tapping forced on-bridge test on the pin–roller bridge using three different springs at three different speeds.

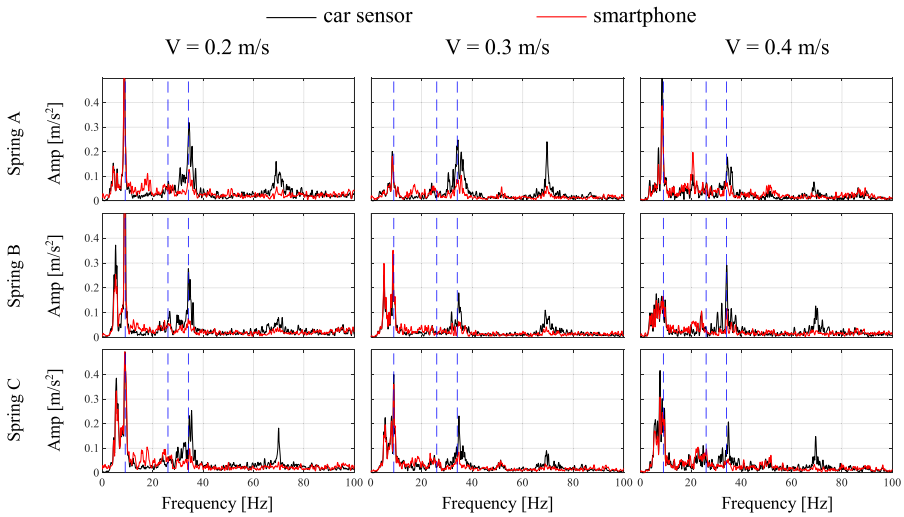

Fig. 14. ADFT spectrum of the car sensor and smartphone under tapping forced on-bridge test on the fixed–fixed bridge using three different springs at three different speeds.

To investigate the potential of the framework presented in this paper for damage detection of bridges, analysis results presented in the previous sections are compared in Fig. 15. The organization of Fig. 15 is similar to previous figures containing all cases of different suspension systems at different speeds. However, each graph contains three curves: off-bridge spectrum with a black solid line, on-bridge spectrum over the pin–roller bridge with a red solid line, and on-bridge spectrum over the fixed–fixed bridge with a blue solid line, all using recorded signals with the smartphone. In addition, the exact values of the fundamental frequencies of both bridges are shown using dashed lines, i.e., a red line for the pin–pin bridge and a blue line for the fixed–fixed bridge. Note that a narrow range of 0–20 Hz is selected to concentrate on the fundamental frequency of the bridge in the spectrums.

Fig. 15 shows that if many different vehicles are moving over a bridge, it is possible to identify changes in the frequency of the bridge in most cases, although this deviation is not clearly captured in some cases, especially at higher speeds. The off-bridge spectrum provides a reliable tool to distinguish between car related and bridge related peaks. Although the source and amount of the shift in the frequency of the bridge are still unknown and a subject of contention in the literature, these experiments demonstrate that it is possible to use smartphone data to detect changes in the bridge state, such as boundary conditions. The relatively large mass ratio of the robot car to the bridge in the experiments plays a major role in increasing the shift of the identified frequency since the mass distribution of the system changed as the car passes over the bridge and the frequency tends to be smaller due to larger total weight. It is expected that in real-life practice with a lower mass ratio of a car to bridge, the amount of the shift would be smaller.

To investigate the capability of detecting bridge frequency, the peak picking technique described in the methodology section is applied to the data shown in Fig. 15. The resulting peak scores are

J. Bridge Eng., 2020, 25(7): 04020041

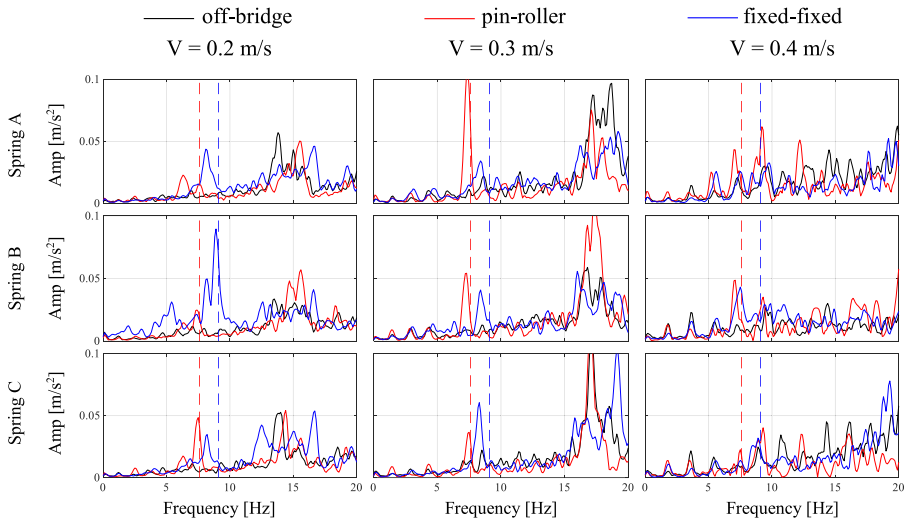

Fig. 15. ADFT spectrum of the smartphone under off-bridge test, on-bridge test over the pin–roller bridge, and on-bridge test over the fixed–fixed bridge using three different springs at three different speeds.

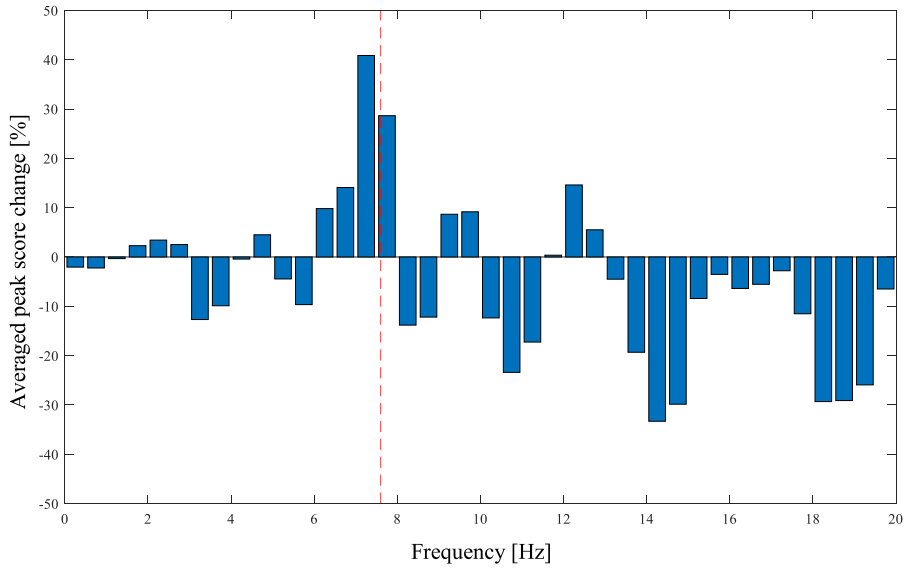

Fig. 16. Averaged peak score change of all passes on the pin–pin bridge versus off-bridge.

then used to find the most probable range for the frequency of both pin–pin and fixed–fixed bridges. For this purpose, successive 0.5 Hz-wide windows are considered in each spectrum and the score of all peaks in those windows are averaged. This averaged score represents the significance of the peaks in each frequency range of that spectrum. Comparing averaged peak scores for each frequency range between two different passes, i.e., off-bridge, pin–pin, or fixed–fixed bridge, makes it possible to detect the frequency range with the largest score change, which represents the frequency range of the corresponding bridge.

This process is conducted on all different combinations of suspension and speed shown in Fig. 15 and the results are shown in Figs. 16–18. The red and blue dashed lines in these figures show the fundamental frequency of pin–pin and fixed–fixed bridges, respectively. Fig. 16 shows the change in the averaged peak score of the pin–pin bridge with respect to the off-bridge condition. As shown, the largest increase in the averaged peak score is in the 7–8 Hz range, which covers the exact frequency of 7.6 Hz. It is expected that most of the bridge related peaks are <7.6 Hz since the shifted frequency is expected to be smaller than the exact frequency. Similarly, Fig. 17 representing the change in the averaged peak score of the fixed–fixed bridge with respect to off-bridge shows the most changes in 7.5–9 Hz, close to 9 Hz of the fundamental frequency of the fixed–fixed bridge.

More insights are provided by comparing the passes over pin–pin and fixed–fixed bridges. Fig. 18 shows the same score change described in Figs. 16 and 17 considering the fixed–fixed bridge as the baseline. As shown, there is a large drop in the averaged peak score of the frequencies near the fixed–fixed bridge, while there is a large increase close to that of the pin–pin bridge. This plot represents the main output of this section, which is bridge state detection. Using the vibration data from different cars with different speeds passing over two different bridge states, this methodology would be able to detect the change in the frequency of those bridges without prior knowledge of their frequency.

It is noted that the resolution and accuracy of the identified frequencies are expected to increase with the use of future smartphones because the quality and performance of the built-in

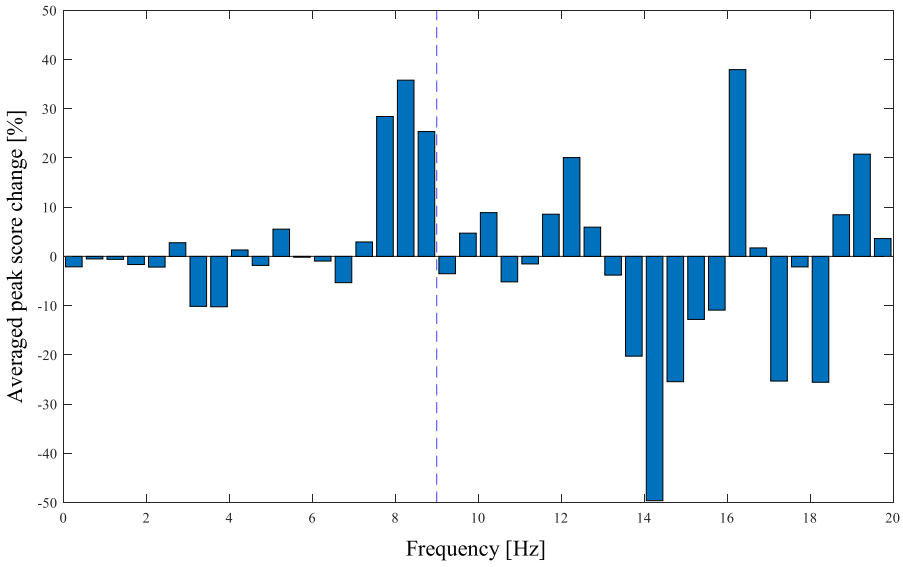

Fig. 17. Averaged peak score change of all passes on the fixed–fixed bridge versus off-bridge.

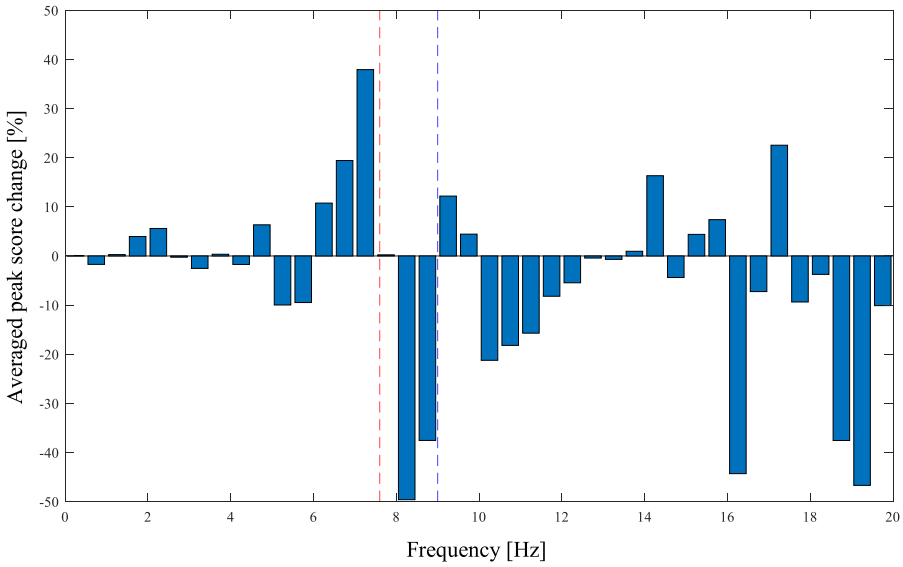

Fig. 18. Averaged peak score change of all passes on the pin–pin bridge versus the fixed–fixed bridge.

sensors in smartphones increased considerably over time. For example, the maximum sampling frequency for a Samsung Galaxy S5 is 200 Hz whereas it is 400 Hz for the Samsung Galaxy S8 used for the experiments presented in this paper. Such developments in technology will further increase the benefits of the framework presented in this paper.

Conclusions

This paper proposes a crowdsensing framework for utilizing smartphone data to evaluate populations of bridges in future smart cities. The analysis framework and experimental results presented in this paper demonstrate that the fundamental frequency and possibly higher mode frequencies of a bridge can be detected by analyzing the vibration data recorded using a smartphone on a vehicle crossing the bridge. Different combinations of the suspension springs and speeds for the vehicle as well as considering two bridges with different support systems provide strong evidence for the robustness of the method against vehicle and bridge properties. In addition, since any severe damage to the bridge would have a significant impact on its fundamental frequency, this study proves that there is a possibility that such damage could be identified through an appropriate crowdsensing framework which gathers data from a large population of smartphones on different cars passing over a bridge. Furthermore, this study shows that even though the identified frequency of the bridge using vibration data of the vehicle is shifted, and the magnitude of this shift is still unknown for different vehicle–bridge systems, it is still possible to successfully detect the frequency change of the bridge. It is noted that the surface roughness is expected to play a significant role in the recorded acceleration signals and its effect on the performance of the proposed methodology needs to be investigated in future studies. The most significant factor on the frequency shift is identified as the speed of the car, which can be recorded through GPS sensor inside the smartphone without the need of installing extra sensors.

Data Availability Statement

Some or all data, models, or codes that support the findings of this study are available from the corresponding author upon reasonable request.

Acknowledgments

The financial support from the corresponding author's Natural Sciences and Engineering Research Council of Canada (NSERC) Discovery Grant is gratefully acknowledged.

References

Adeli, H., and X. Jiang. 2009. *Intelligent infrastructure. Neural networks, wavelets, and chaos theory for intelligent transportation systems and smart structures*. London: CRC Press.

Bhoraskar, R., N. Vankadhara, B. Raman, and P. Kulkarni. 2012. "Wolverine: Traffic and road condition estimation using smartphone sensors." In *Proc., 4th Int. Conf. on Communication Systems and Networks*, 1–6. Piscataway, NJ: IEEE.

Catbas, F. N., M. Gul, and J. L. Burkett. 2008. "Conceptual damage-sensitive features for structural health monitoring: Laboratory and field demonstrations." *Mech. Syst. Sig. Process.* 22 (7): 1650–1669. https://doi.org/10.1016/j.ymssp.2008.03.005.

CCA/CPWA/CSCE/FCM (Canadian Construction Association, Canadian Public Works Association, Canadian Society for Civil Engineering, Federation of Canadian Municipalities). 2019. *Informing the future: Assessing the health of our communities' infrastructure*. Canadian Infrastructural Rep. Card 2016. Ottawa, Canada: Canadian Infrastructure Report Card (CIRC).

Cerda, F., S. Chen, J. Bielak, J. H. Garrett, P. Rizzo, and J. Kovačević. 2014. "Indirect structural health monitoring of a simplified laboratory-scale bridge model." *Smart Struct. Syst.* 13 (5): 849–868. https://doi.org/10.12989/sss.2014.13.5.849.

Chourabi, H., T. Nam, S. Walker, J. R. Gil-Garcia, S. Mellouli, K. Nahon, T. A. Pardo, and H. J. Scholl. 2012. "Understanding smart cities: An integrative framework." In *Proc., Annual Hawaii Int. Conf. on System Sciences*, 2289–2297. Piscataway, NJ: IEEE.

Feng, M., Y. Fukuda, M. Mizuta, and E. Ozer. 2015. "Citizen sensors for SHM: Use of accelerometer data from smartphones." *Sensors* 15 (2): 2980–2998. https://doi.org/10.3390/s150202980.

Glancy, D. J. 2014. "Sharing the road: Smart transportation infrastructure." *Fordham Urban Law J.* 41: 1617–1664.

Graham, S. 2010. *Disrupted cities: When infrastructure fails*. New York: Routledge.

Guan, S., J. A. Bridge, C. Li, and N. J. DeMello. 2019. "Smart radar sensor network for bridge displacement monitoring." *J. Bridge Eng.* 24 (1): 04018102. https://doi.org/10.1061/(ASCE)BE.1943-5592.0001322.

Gul, M., and F. N. Catbas. 2009. "Statistical pattern recognition for structural health monitoring using time series modeling: Theory and experimental verifications." *Mech. Syst. Sig. Process.* 23 (7): 2192–2204. https://doi.org/10.1016/j.ymssp.2009.02.013.

Ham, H., T. J. Kim, and D. Boyce. 2005. "Assessment of economic impacts from unexpected events with an interregional commodity flow and multimodal transportation network model." *Transp. Res. A Policy Pract.* 39 (10): 849–860. https://doi.org/10.1016/j.tra.2005.02.006.

Händel, P., J. Ohlsson, M. Ohlsson, I. Skog, and E. Nygren. 2014. "Smartphone-based measurement systems for road vehicle traffic monitoring and usage-based insurance." *IEEE Syst. J.* 8 (4): 1238–1248. https://doi.org/10.1109/JSYST.2013.2292721.

Harris, F. J. 1978. "On the use of windows for harmonic analysis with the discrete Fourier transform." *Proc. IEEE* 66 (1): 51–83. https://doi.org/10.1109/PROC.1978.10837.

Hattori, H., X. He, F. N. Catbas, H. Furuta, and M. Kawatani. 2012. "A bridge damage detection approach using vehicle-bridge interaction analysis and neural network technique." In *Bridge maintenance, safety, management, resilience and sustainability*, edited by F. Biondini and D. M. Frangopol, 376–383. London: CRC Press.

Hester, D., and A. González. 2017. "A discussion on the merits and limitations of using drive-by monitoring to detect localised damage in a bridge." *Mech. Syst. Sig. Process*. 90: 234–253. https://doi.org/10.1016/j.ymssp.2016.12.012.

Hoult, N. A., P. R. A. Fidler, P. G. Hill, and C. R. Middleton. 2010. "Long-term wireless structural health monitoring of the ferriby road bridge." *J. Bridge Eng.* 15 (2): 153–159. https://doi.org/10.1061/(ASCE)BE.1943-5592.0000049.

Hsieh, K. H., M. W. Halling, and P. J. Barr. 2006. "Overview of vibrational structural health monitoring with representative case studies." *J. Bridge Eng.* 11 (6): 707–715. https://doi.org/10.1061/(ASCE)1084-0702(2006)11:6(707).

Keenahan, J., E. J. OBrien, P. J. McGetrick, and A. Gonzalez. 2014. "The use of a dynamic truck-trailer drive-by system to monitor bridge damping." *Struct. Health Monit.* 13 (2): 143–157. https://doi.org/10.1177/1475921713513974.

Kim, C., R. Isemoto, T. Toshinami, M. Kawatani, P. McGetrick, and E. J. O'Brien. 2011. "Experimental investigation of drive-by bridge inspection." In *Proc., 5th Int. Conf. on Structural Health Monitoring of Intelligent Infrastructure*, 1–9. Cancun, Mexico: Instituto de Ingeniería, UNAM.

Kim, J., and J. P. Lynch. 2012. "Experimental analysis of vehicle-bridge interaction using a wireless monitoring system and a two-stage system identification technique." *Mech. Syst. Sig. Process.* 28: 3–19. https://doi.org/10.1016/j.ymssp.2011.12.008.

Ko, J. M., and Y. Q. Ni. 2005. "Technology developments in structural health monitoring of large-scale bridges." *Eng. Struct.* 27 (12): 1715–1725. https://doi.org/10.1016/j.engstruct.2005.02.021.

Kong, Q., R. M. Allen, M. D. Kohler, T. H. Heaton, and J. Bunn. 2018. "Structural health monitoring of buildings using smartphone sensors." *Seismol. Res. Lett.* 89 (2A): 594–602. https://doi.org/10.1785/0220170111.

Li, J., X. Zhu, S. Law, and B. Samali. 2019. "Drive-by blind modal identification with singular spectrum analysis." *J. Aerosp. Eng.* 32 (4): 04019050. https://doi.org/10.1061/(ASCE)AS.1943-5525.0001030.

Lin, C. W., and Y. B. Yang. 2005. "Use of a passing vehicle to scan the fundamental bridge frequencies: An experimental verification." *Eng. Struct.* 27 (13): 1865–1878. https://doi.org/10.1016/j.engstruct.2005.06.016.

Malekjafarian, A., P. J. McGetrick, and E. J. OBrien. 2015. "A review of indirect bridge monitoring using passing vehicles." *Shock Vib.* 2015: 286139.

Matarazzo, T. J., P. Santi, S. N. Pakzad, K. Carter, C. Ratti, B. Moaveni, C. Osgood, and N. Jacob. 2018. "Crowdsensing framework for monitoring bridge vibrations using moving smartphones." *Proc. IEEE* 106 (4): 577–593. https://doi.org/10.1109/JPROC.2018.2808759.

Mei, Q., and M. Gül. 2019. "A crowdsourcing-based methodology using smartphones for bridge health monitoring." *Struct. Health Monit.* 18 (5–6): 1602–1619. https://doi.org/10.1177/1475921718815457.

Mei, Q., M. Gül, and M. Boay. 2019. "Indirect health monitoring of bridges using Mel-frequency cepstral coefficients and principal component analysis." *Mech. Syst. Sig. Process.* 119: 523–546. https://doi.org/10.1016/j.ymssp.2018.10.006.

Mohan, P., V. N. Padmanabhan, and R. Ramjee. 2008. "Nericell: Rich monitoring of road and traffic conditions using mobile smartphones." In *Proc., 6th ACM Conf. on Embedded Network Sensor Systems*, 323–336. New York: Association for Computing Machinery.

Morgenthal, G., S. Rau, J. Taraben, and T. Abbas. 2018. "Determination of stay-cable forces using highly mobile vibration measurement devices." *J. Bridge Eng.* 23 (2): 04017136. https://doi.org/10.1061/(ASCE)BE.1943-5592.0001166.

OBrien, E. J., A. Malekjafarian, and A. González. 2017. "Application of empirical mode decomposition to drive-by bridge damage detection." *Eur. J. Mech.* 61: 151–163. https://doi.org/10.1016/j.euromechsol.2016.09.009.

Ozer, E., and M. Q. Feng. 2016. "Synthesizing spatiotemporally sparse smartphone sensor data for bridge modal identification." *Smart Mater. Struct.* 25 (8). https://doi.org/10.1088/0964-1726/25/8/085007.

Ozer, E., and M. Q. Feng. 2017. "Direction-sensitive smart monitoring of structures using heterogeneous smartphone sensor data and coordinate system transformation." *Smart Mater. Struct.* 26 (4): 045026. https://doi.org/10.1088/1361-665X/aa6298.

Siringoringo, D. M., and Y. Fujino. 2012. "Estimating bridge fundamental frequency from vibration response of instrumented passing vehicle: Analytical and experimental study." *Adv. Struct. Eng.* 15 (3): 417–433. https://doi.org/10.1260/1369-4332.15.3.417.

Washburn, D., U. Sindhu, S. Balaouras, R. Dines, N. Hayes, and L. Nelson. 2010. *Helping CIOs understand 'smart city' initiatives*. Cambridge, MA: Forrester Research.

Welch, P. D. 1967. "The use of fast Fourier transform for the estimation of power spectra: A method based on time averaging over short, modified periodograms." *IEEE Trans. Audio Electroacoust.* 15 (2): 70–73. https://doi.org/10.1109/TAU.1967.1161901.

Wenzel, H. 2008. *Health monitoring of bridges*. Chichester: John Wiley & Sons.

Wong, K.-Y. 2004. "Instrumentation and health monitoring of cable-supported bridges." *Struct. Control Health Monit.* 11 (2): 91–124. https://doi.org/10.1002/stc.33.

Xiong, Z., H. Sheng, W. G. Rong, and D. E. Cooper. 2012. "Intelligent transportation systems for smart cities: A progress review." *Sci. China Inform. Sci.* 55 (12): 2908–2914. https://doi.org/10.1007/s11432-012-4725-1.

Yang, Y. B., and W. F. Chen. 2016. "Extraction of bridge frequencies from a moving test vehicle by stochastic subspace identification." *J. Bridge Eng.* 21 (3): 04015053. https://doi.org/10.1061/(ASCE)BE.1943-5592.0000792.

Yang, Y. B., C. W. Lin, and J. D. Yau. 2004. "Extracting bridge frequencies from the dynamic response of a passing vehicle." *J. Sound Vib.* 272 (3–5): 471–493. https://doi.org/10.1016/S0022-460X(03)00378-X.

Yang, Y. B., and J. D. Yau. 1997. "Vehicle-bridge interaction element for dynamic analysis." *J. Struct. Eng.* 123 (11): 1512–1518. https://doi.org/10.1061/(ASCE)0733-9445(1997)123:11(1512).

Zhang, Y., S. T. Lie, and Z. Xiang. 2013. "Damage detection method based on operating deflection shape curvature extracted from dynamic response of a passing vehicle." *Mech. Syst. Sig. Process.* 35 (1–2): 238–254. https://doi.org/10.1016/j.ymssp.2012.10.002.

Zhao, X., R. Han, Y. Yu, W. Hu, D. Jiao, X. Mao, M. Li, and J. Ou. 2017. "Smartphone-based mobile testing technique for quick bridge cable-force measurement." *J. Bridge Eng.* 22 (4): 06016012. https://doi.org/10.1061/(ASCE)BE.1943-5592.0001011.